Solar Energy 228 (2021) 339–348

Contents lists available at ScienceDirect

Solar Energy

journal homepage: www.elsevier.com/locate/solener

Performance analysis of the aerogel-based PV/T collector: A numerical study

Lijun Wu, Bin Zhao *, Xianze Ao, Honglun Yang, Xiao Ren, Qiongwan Yu, Ke Guo, Maobin Hu, Gang Pei *

Department of Thermal Science and Energy Engineering, University of Science and Technology of China, Hefei 230027, China

ARTICLE INFO

Keywords:
Solar energy
Silica aerogel
Heat loss
Thermal radiation
PV/T

ABSTRACT

Photovoltaic/thermal (PV/T) collector can convert incident sunlight into electrical and heat energy simultaneously. However, compared with the solar thermal collector, the radiative heat loss of the PV/T absorber is larger since the spectrally selective PV/T absorber is difficult to design and fabricate after introducing PV cells, which leads to lower thermal efficiency. Thus, an approach that can reduce the radiative heat loss of the PV/T collector without the requirement for spectrally selective PV/T absorber is emergently needed. Here, a novel aerogel-based PV/T collector is proposed to suppress radiative heat loss and improve efficiency by introducing the silica aerogel that is highly transparent to sunlight and opaque to infrared light, as well as ultra-low effective thermal conductive into the PV/T collector. A numerical model is established to evaluate the performance of the aerogel-based PV/T collector, and the results present that the heat loss of the PV/T collector at the operating temperature of 70°C can be dramatically reduced by approximately 75% after using the silica aerogel and the thermal efficiency can also be increased by 46%. Moreover, a parametric study is conducted to investigate the influence of solar radiation, ambient temperature, and emissivity of the PV/T absorber on the performance of the aerogel-based PV/T collector. This study is devoted to exploring a new method to suppress the radiative heat loss of the PV/T collector and enhance its solar harvesting performance correspondingly, which gives a reference for the design of high-performance PV/T utilization.

1. Introduction

In the 1970s, the photovoltaic/thermal (PV/T) collector was proposed due to its high overall solar conversion efficiency (Wolf, 1976). However, the thermal efficiency of the PV/T collector is significantly lower than that of the solar thermal collector under the same conditions. Besides, the thermal efficiency of the PV/T collector drops drastically as the operating temperature increases. The main reason for this phenomenon is that the PV/T absorber cannot achieve spectral selectivity. The function of the spectral selectivity absorber is to achieve high absorption of solar energy in the 0.3–2.5 μm band to obtain a high solar absorption rate, and low thermal emissivity in the 2.5–50 μm band to reduce its radiative heat loss (Burlafinger et al., 2015). As illustrated in Fig. 1, the solar collector can achieve higher thermal efficiency at a high operating temperature, because its emissivity is much lower than the PV/T absorber in the 2.5–20 μm band. As early as ten years ago, researchers proposed a spectral selective PV/T absorber by adding an optical coating to suppress the radiative loss and improve its overall efficiency (Cox Iii and Raghuraman, 1985; van Helden et al., 2004). However, the coating was not transparent enough to meet the requirement for electricity generation. So, the PV/T collector with excellent spectral selectivity has not yet appeared.

The low thermal efficiency of the PV/T collector is caused by a high radiative loss in the infrared band and this is because the PV/T absorber cannot achieve spectral selectivity. Thus, the market of PV/T collectors is focused on low-temperature level applications in buildings, such as space heating, domestic hot water, and electricity generation. For instance, Ji et al. (2011) conducted a dual-function solar collector combined with the buildings to provide heat energy for space heating and domestic hot water in cold and warm seasons, respectively. The previously reported research has shown that the hybrid PV/T system can efficiently provide electricity and serve as a heat source of domestic hot water simultaneously, the economy of the system has been greatly improved (Kalogirou and Tripanagnostopoulos, 2006).

In the previously published literature, the main method is to reduce

* Corresponding authors.
E-mail addresses: zb630@ustc.edu.cn (B. Zhao), peigang@ustc.edu.cn (G. Pei).

https://doi.org/10.1016/j.solener.2021.09.077
Received 21 June 2021; Received in revised form 24 September 2021; Accepted 25 September 2021
Available online 30 September 2021

Nomenclature

I	Radiative intensity field, W/m^2
P	Phase function
k	Thermal conductivity of silica aerogel, W/m/K
T	Temperature, °C
q	Spatial radiative heat flux, W/m^2
Q_{loss}	Total thermal loss, W/m^2
Q_{rec}	Incident solar radiation, W/m^2
Q_{abs}	The heat flux absorbed by PV/T absorber, W/m^2
$Price_{el}$	Price of electrical energy, USD/kWh
$Price_{th}$	Price of thermal energy, USD/kWh
R	Annual money saving, USD
R_y	Money-saving during the useful life, USD
m	The complex refractive index of silica
f_v	The volume fraction of the silica particles
d	The diameter of the silica particles in the aerogel, nm
E	The output power density of the PV/T collector, W/m^2
A	The area of the PV/T collector, m^2

Subscripts and abbreviations

DOM	Discrete coordinate method
RTE	Radiative transfer equation
Amb	Ambient
PV/T	Photovoltaic/thermal
a	Aerogel layer
th	Thermal energy
ad	Adhesive

Greek letters

τ	Transmittance
η	Energy efficiency
α	Absorptivity
β	Temperature coefficient of the PV cell, K^{-1}
κ	Absorption coefficient, m^{-1}
λ	Wavelength, nm
σ	Scattering coefficient, m^{-1}
ζ	Packing factor

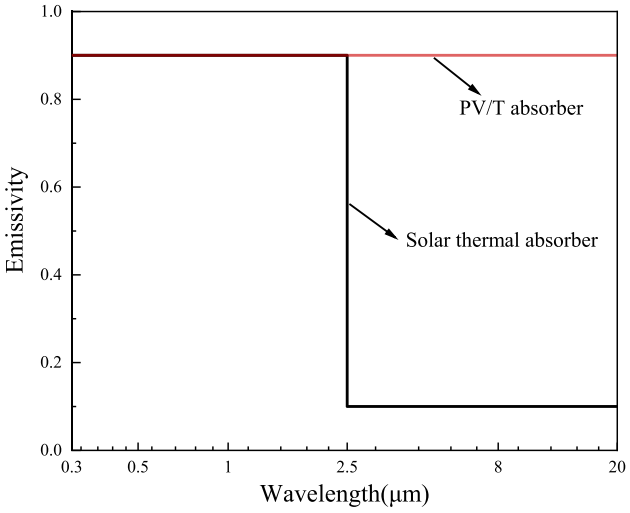

Fig. 1. The emissivity of the solar thermal absorber and PV/T absorber.

heat conduction, convection between the PV/T absorber and environment to improve the overall efficiency. For instance, adding a glass cover to suppress heat convection between PV/T absorber and environment is the most common method. The reported experiment and simulation results confirmed that the solar energy conversion efficiency of the PV/T collector with a glass cover is always higher than that of the PV/T collector without a glass cover (Chow et al., 2009). Although convection and thermal conduction losses are reduced after adding glass cover, radiative heat loss still exists and accounts for the majority of heat loss in this condition since the radiation power of the PV/T absorber is proportional to the fourth power of its temperature. Under this condition, using the spectrally selective absorber is an alternative technology to reduce radiative loss without affecting the absorption of the solar spectrum, which has already been widely used in solar thermal collectors (Ehrmann and Reineke-Koch, 2012). For the PV/T collector, due to the difficulty in designing and manufacturing spectrally selective absorbers after the introduction of PV cells, there are few studies on spectrally selective PV/T absorbers. In this regard, an alternative solution is proposed to minimize the radiative loss caused by PV/T absorber by using a kind of low thermally conductive material that is transparent to the solar radiation but opaque to the infrared radiation to replace the gap between the PV/T absorber and glass envelope. What's more, when the air gap is occupied by material with low thermal conductivity, the heat transfer (conduction and convection) between hot PV/T absorber and environment is suppressed.

The silica aerogel is a kind of potential thermally insulating material that can be used for solar harvesting (Benz et al., 1996; Gunay et al., 2018). Traditional aerogels are usually used in building windows. When its thickness is 10 mm, its transmittance to the sun is usually low, less than 60%. If those aerogels are used in PV/T collector, the high optical loss caused by the scattering will result in a significant decrease in the amount of incident sunlight and negates its thermal insulation, the electricity generation by the PV cell is reduced. Consequently, the aerogel has not been used in the PV/T collector. In 2017, Strobach et al. (2017) optimized the manufacturing process of aerogel to improve its ability to transmit sunlight. The sunlight transmittance of the silica aerogel can achieve up to 96% at the thickness of 9.5 mm. Besides, Zhao et al. (2019, 2020) optimized the microstructure of the aerogel to reduce scattering and the transmittance of the silica aerogel is up to 95%. Thus, the silica aerogel layer can achieve high solar transmission and low infrared radiation transmission, so that the negative impact of silica aerogel optical loss on PV cell electricity generation can be minimized and the radiative loss can be reduced. Besides, silica aerogel is mesoporous material so that its thermal conductivity could be optimized to be lower than that of air (25 mW/m/K (Tang et al., 2008)).

According to the above analysis, radiative heat loss caused by the high emissivity of the PV/T absorber makes the efficiency at a low level. Therefore, a new PV/T absorber by coating PV cells with silica aerogel is proposed to improve the efficiency of the PV/T collector by diminishing the radiative loss. Besides, there is a knowledge gap on the topic of introducing the silica aerogel into the PV/T collector to enhance the thermal performance, and a further study of the performance of the aerogel-based PV/T collector under different working conditions is also needed. Under this context, a combined optical-thermal-electrical model is developed to assess the performance of silica aerogel-based PV/T collector. First, the transmittance of the silica aerogel layer under different thicknesses and the heat loss of the different PV/T collectors are investigated, respectively. Second, the thermal and electrical efficiencies of the aerogel-based PV/T collector are evaluated and compared with the traditional PV/T collector. Finally, a parametric study is conducted to investigate the influence of incident radiation, ambient temperature, and coating emissivity on the performance of the aerogel-based PV/T collector.

2. Methodology

2.1. Mathematical model

The collector is composed of an aerogel layer, a PV/T absorber (composed of the polycrystalline silicon PV cell, TPT, EVA, and cell substrate), and an insulation layer. The schematic of the aerogel-based PV/T collector is illustrated in Fig. 2. Incident radiation that passes through the aerogel layer is absorbed and converted into useful heat Q_{th} and electricity E_{pv} by PV/T absorber. The reflection of the aerogel layer and the scattering of the aerogel layer reduces a small fraction of solar radiation reaching the PV/T absorber. The silica aerogel layer can absorb thermal radiation from the PV/T absorber and re-emitted part of it back to the PV/T absorber, resulting in an enormous radiation loss reduction of the PV/T absorber. To accurately calculate the radiation transmission within the aerogel, we use the radiative transfer equation (RTE) that describes the radiative intensity filed as the function of position (determined by a position vector $\vec{z}$) and a direction (determined by a unit direction vector $\vec{s}$), and wavelength(λ). The RTE is described as (Modest, 2013):

$$\frac{dI_\lambda(z,\vec{s})}{dz} = \kappa_\lambda I_{b\lambda}(z) - (\sigma_\lambda + \kappa_\lambda) I_\lambda(z,\vec{s}) + \frac{\sigma_\lambda}{4\pi}\int_{4\pi} I'_\lambda(z,\vec{s}) P_\lambda(\vec{s}', \vec{s}) d\Omega' \tag{1}$$

where I_λ is the radiative intensity field, σ_λ and κ_λ represent scattering coefficient absorption coefficient, respectively. $I_{b\lambda}$ represents the blackbody intensity coupled with the temperature filed within the aerogel, $P_\lambda(\vec{s}', \vec{s})$ is the phase function which is assumed to be isotropic in this paper and this assumption has already been used and validated (Li et al., 2015; Tang et al., 2015). In this paper, radiation is divided into the solar radiation band ($\lambda < 2.5$ μm) and the thermal radiation band ($\lambda > 2.5$ μm).

In the solar radiation band ($\lambda < 2.5$ μm), the blackbody intensity $I_{b\lambda}$ can be negligible, because the aerogel's temperature is much lower than the sun's temperature (Gunay et al., 2018). Therefore, the RTE is decoupled with temperature, and Eq. (1) can be simplified as:

$$\frac{dI_\lambda(z,\vec{s})}{dz} = -(\sigma_\lambda + \kappa_\lambda) I_\lambda(z,\vec{s}) + \frac{\sigma_\lambda}{4\pi}\int_{4\pi} I'_\lambda(z,\vec{s}) d\Omega' \tag{2}$$

In the thermal radiation band ($\lambda > 2.5$ μm), $I_{b\lambda}$ can't be negligible since the emission intensity of the aerogel is mainly concentrated in the thermal band. Therefore, the RTE should be solved by coupling with the temperature field.

$$k\frac{d^2T}{dz^2} - \frac{dq^r_{\lambda=0\sim\infty}}{dz} = 0 \tag{3}$$

k represents the solid thermal conductivity of the silica aerogel, $q^r_{\lambda=0\sim\infty}$ represents the spatial radiative heat flux obtained by RTE, which can be described as:

$$q^r_{\lambda=0\sim\infty} = \int_0^\infty \int_{4\pi} I_\lambda(\vec{s})\vec{s}\, d\Omega d\lambda \tag{4}$$

After the radiation field is calculated, the transmittance of the aerogel can be obtained. In the aerogel, the AM1.5 ("AM1.5″, 1.5-atmosphere thickness, corresponds to a solar zenith angle of 48.2°, and the solar irradiance is 1000 W/m^2) weighted transmittance can be used, which can be calculated by Zhao et al. (2016):

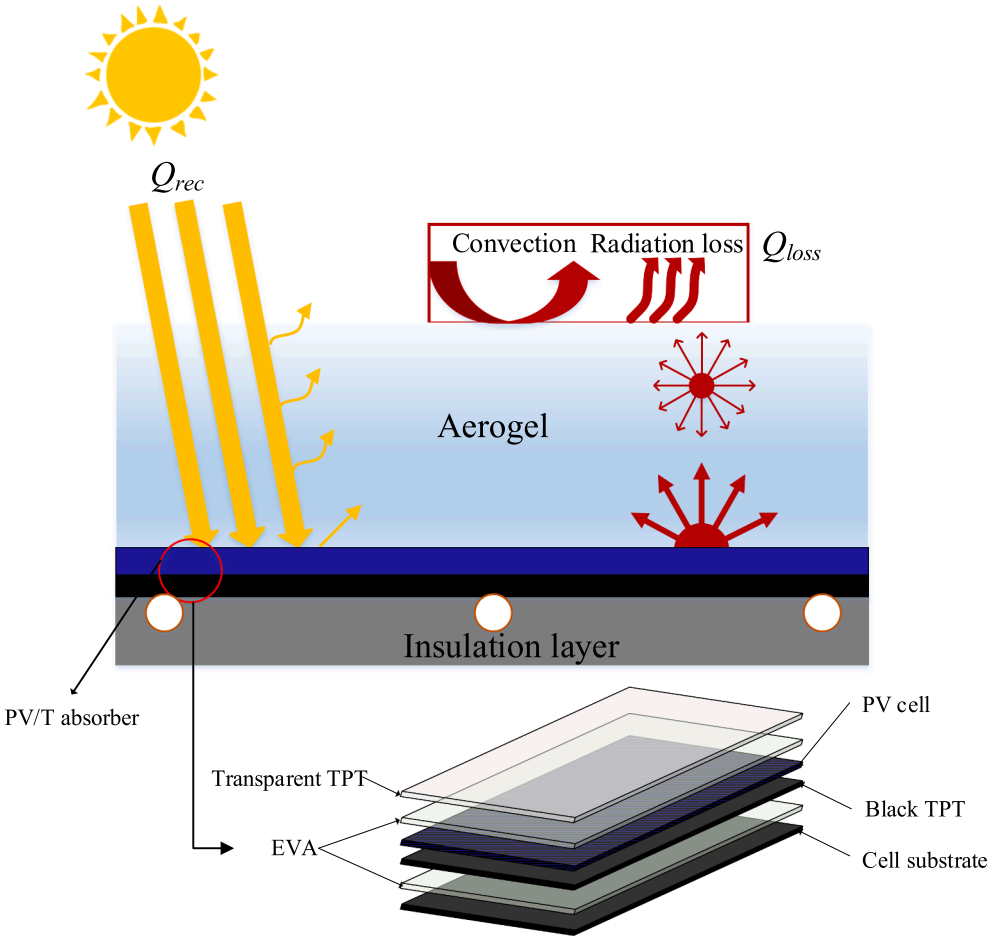

Fig. 2. Schematic of the aerogel-based PV/T collector.

$$\tau_a = \frac{\int I_{AM1.5}(\lambda)\tau_{(AM1.5)}(\lambda)d\lambda}{\int I_{AM1.5}(\lambda)d\lambda} \quad (5)$$

the numerator is the total transmitted radiation of AM1.5, and the denominator is the total radiation of AM1.5.

The thermal efficiency of the PV/T collector is the function of the heat loss and solar radiation absorbed by the PV/T absorber, which can be calculated by McEnaney et al. (2017):

$$\eta_{th} = \frac{Q_{abs} - Q_{loss}}{Q_{rec}} \quad (6)$$

where Q_{loss} represents the total heat loss of PV/T collector; Q_{rec} is the incident solar radiation; Q_{abs} is the incident solar radiation absorbed by PV/T absorber, which is determined by (Bhattarai et al., 2012):

$$Q_{abs} = Q_{rec}\tau_a\tau_{ad}\alpha - \zeta E_{pv} \quad (7)$$

where τ_{ad} and τ_a represent the transmittances of adhesive, and the aerogel layer, respectively; ζ denote the packing factor of the PV cells, α means the comprehensive absorption of the PV/T absorber which is expressed as:

$$\alpha = \alpha_p\zeta + \alpha_b(1-\zeta) \quad (8)$$

α_p and α_b are the absorptivities of the PV/T absorber with and without PV cells; E_{pv} means the output power density of the PV/T collector which can be calculated by (Yu et al., 2020):

$$E_{pv} = Q_{rec}\tau_a\tau_{ad}\eta_{e,ref}[1 - \beta_{pv}(T - T_{ref})] \quad (9)$$

$\eta_{e,ref}$ denotes the efficiency of PV cell under the standard testing condition ($T_{ref} = 25°C$, 1000 W/m^2) and it was taken from ref (Al-Waeli et al., 2017), β_{pv} is −0.4%/K that is the typical value of the temperature coefficient of the polycrystalline silicon PV cell (Dubey et al., 2013). At present, the electrical efficiency decreases as the temperature rising, which is caused by the negative temperature coefficient of the PV cell. However, with the development of the new generation of PV cells that have positive temperature coefficients, such as cells reported in ref. (Huang et al., 2019), the output power of the PV cell will be improved with increased operating temperature.

The electrical efficiency η_e is expressed as:

$$\eta_e = \frac{E_{pv}}{Q_{rec}} \quad (10)$$

Generally, the energy grade of the electricity is higher than the grade of the thermal energy, thus the total efficiency of the PV/T collector is not the simple accumulation of the electrical efficiency and thermal efficiency. In this paper, the thermal energy is assumed to be converted into thermal exergy and the thermal exergy efficiency is described as (Du et al., 2019):

$$\eta_{ex,th} = \frac{(1 - \frac{T_{amb}}{T_{pv}})\cdot Q_{th}}{Ex_G} \quad (11)$$

where T_{pv} denotes the temperature of PV cells, T_{amb} is ambient temperature.

The electrical exergy efficiency is defined as:

$$\eta_{ex,pv} = \frac{Ex_{pv}}{Ex_G} = \frac{E_{pv}}{Ex_G} \quad (12)$$

The exergy content of the incident radiation is calculated by:

$$Ex_G = Q_{rec}(1 - \frac{T_{amb}}{T_{sun}}) \quad (13)$$

where $T_{sun} = 5760$ K is the apparent solar temperature (Ren et al., 2021).

Then, the overall exergy efficiency is defined as:

$$\eta_{ex,pv/t} = \zeta\eta_{ex,pv} + \eta_{ex,th} \quad (14)$$

2.2. Economic analysis

In order the investigate the economic feasibility of the aerogel-based PV/T collector, an economic analysis is developed, the price of the electricity and thermal energy is taken into account, and the economic saving during the useful life of the collector is analyzed. The annual saving is calculated by Gagliano et al. (2019):

$$R_y = E_{pv}\cdot A\cdot Price_{el} + (Q_{th} - Q_{aux})\cdot A\cdot Price_{th} \quad (15)$$

where $Price_{el}$ and $Price_{th}$ represent the cost of electricity and thermal energy per kWh, A is the area of collector, Q_{aux} is auxiliary heater energy when the stored energy is not sufficient to meet the demand for hot water.

Their discounted sum is calculated by (Gagliano et al., 2019):

$$R = R_y\frac{(1+r)^n - 1}{r\cdot(1+r)^n} \quad (16)$$

where r represents the capitalization rate which is set as 3%, n is the projection of the useful life which is set of 20 years.

2.3. Optical parameters of the silica aerogel layer

The scattering and absorption coefficients of the silica aerogel layer are related to the porosity of the aerogel, the diameter of the silica particles within the aerogel, and the wavelength of radiation. In this study, silica particles are assumed as sphere particles and the scattering process of silica particles is independent of each other, which is a reasonable hypothesis and it has been proved in ref. (He and Xie, 2015; Tang et al., 2015). The scattering coefficients σ_λ and absorption coefficients κ_λ are expressed as (Mishchenko et al., 2002):

$$\sigma_\lambda = 4\pi^4 f_v\left|\frac{m^2-1}{m^2+2}\right|^2\frac{d^3}{\lambda^4} \quad (17)$$

$$\kappa_\lambda = -\Im\left\{\frac{m^2-1}{m^2+2}\right\}\frac{6\pi f_v}{\lambda} \quad (18)$$

where d is the diameter of the silica particles in the aerogel; f_v represents the volume fraction of the silica particles; λ denotes wavelength; m is the complex refractive index of silica obtained from ref (Palik, 1998).

2.4. Numerical solution

Since the scattering term in Eq. (1) and the radiative intensity of the silica aerogel is the fourth power of the temperature field, it is difficult to obtain its analytical solution. Therefore, the discrete coordinate method (DOM) is used to solve the problem in this paper. First, Eq. (1) is numerically solved by DOM with the corresponding boundary conditions. Then, after obtaining the radiative intensity within the aerogel, the radiative flux can be obtained by Eq. (4). The divergence of the radiative flux is put into Eq. (3) as the heat generation term. Eq. (4) should be solved with the boundary conditions to obtain temperature filed within the aerogel. The iterations were not stopped until $\frac{|T_{i+1}-T_i|}{T_i} \leqslant 10^{-4}$. The detailed process is shown in Fig. 3 and the numerical model is carried out using the MATLAB code.

2.5. Model validation

To validate the radiative and conductive heat transfer within the silica aerogel, the comparative study between the current simulation results and experimental results from reported research developed by Heinemann et al. (1996) is carried out. The thickness of the aerogel is

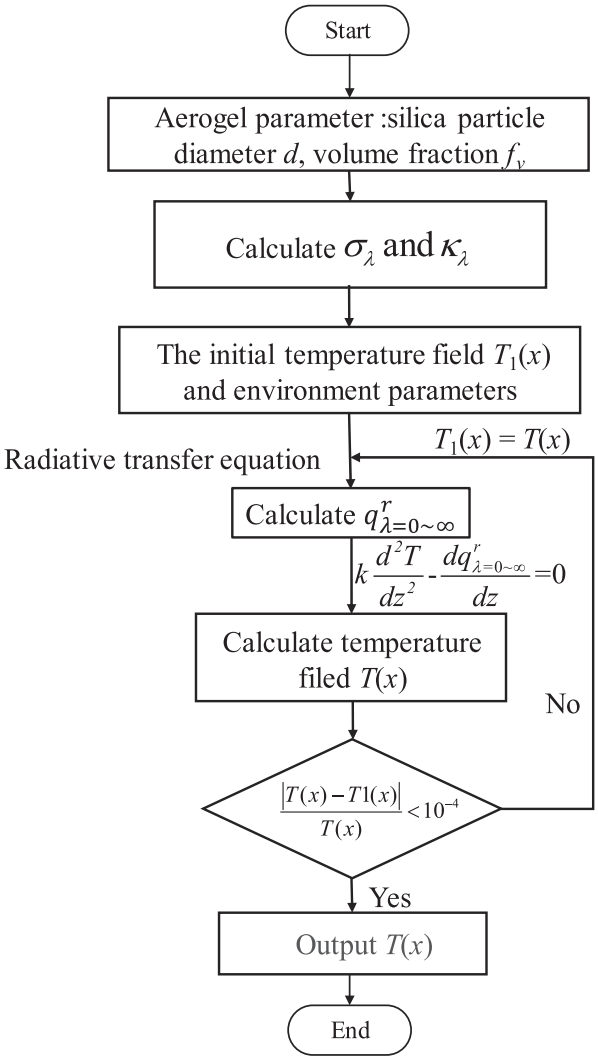

Fig. 3. Flowchart of the heat transfer simulation.

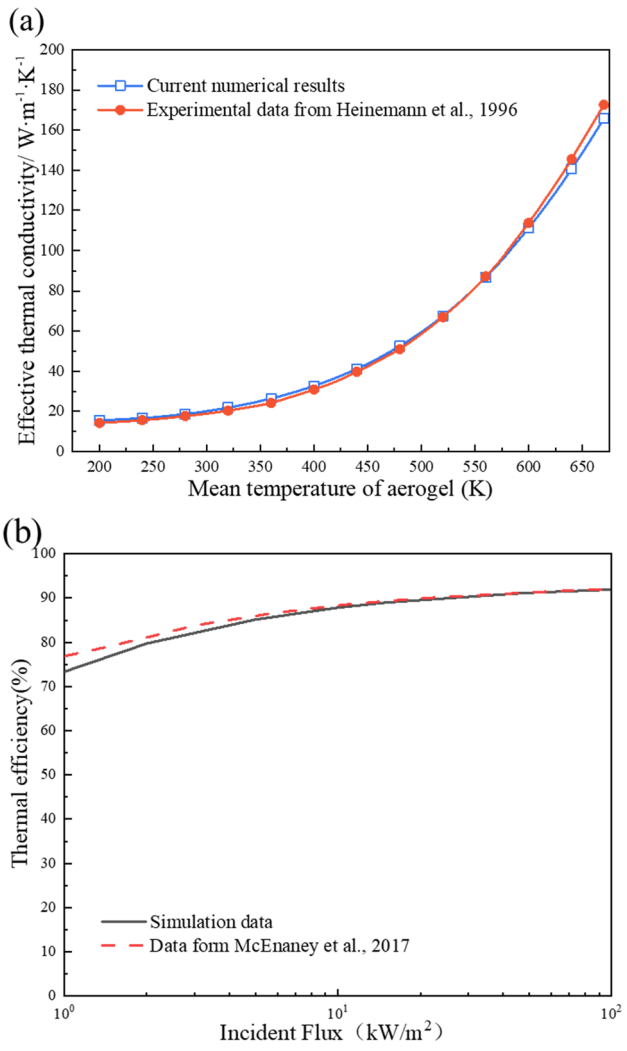

Fig. 4. (a) Simulated effective thermal conductivity compared to the experimental data. (b) The simulated thermal efficiency of the aerogel-based PV/T collector at the absorber temperature of 100°C using the current model and previously published model (McEnaney et al., 2017).

7.9 mm and the density of the aerogel is 220 kg·m^{-3}, and all boundary conditions and parameters are the same as those of ref (Heinemann et al., 1996). The simulation results of the effective thermal conductivity of the aerogel slab under different mean temperatures of aerogel are shown in Fig. 4(a). It is observed that the simulation results are in good agreement with the experimental results, and the relative difference <8.8% in the whole temperature range, which validates the current model.

Moreover, to validate the model of the PV/T collector, a previously reported case (McEnaney et al., 2017) is simulated using the current model and the simulated results are compared with the original data from the case. During the simulation, the input parameters of the glass, aerogel, and boundary conditions are the same as those in ref (McEnaney et al., 2017). As shown in Fig. 4(b), it can be found that the simulated results predicted using the current model is very close to that reported in ref (McEnaney et al., 2017) with a maximum relative error of 4%, and the small difference between simulation results and data from literature is likely caused by the simplification of the model. The reasonable agreement and the slightly relative error show that the model is reliable for performance prediction.

3. Results and discussions

In this sub-section, the aerogel properties and performance of the aerogel-based PV/T collector are first investigated. Then, the effects of ambient temperature and incident radiation on the performance of the aerogel-based PV/T collector are analyzed and the performance of the aerogel-based PV/T collector with selective surface and the non-selective surface is investigated. Finally, the economic analysis of the aerogel-based PV/T collector is investigated.

3.1. The transmittance of the silica aerogel layer

The simulated transmittance of the bulk silica aerogel layer in the wavelength range from 0.3 μm to 20 μm is shown in Fig. 5(a). It can be observed that the silica aerogel layer is transparent to solar radiation but opaque to mid-infrared radiation. To explore the effect of the thickness of the silica aerogel layer and the diameter of silica particles in the silica aerogel layer on its solar transmittance, the transmittance of the silica aerogel layer is calculated under the different thickness of the silica aerogel layer and diameters of silica particles. The simulated results (i.e., the AM1.5 weighted transmittance of the silica aerogel) are presented in Fig. 5(b). It has been found that the transmittance of the silica aerogel layer decreases with the increased thickness of the aerogel layer and the diameter of silica particles. For instance, when silica particles diameter d is 6 nm, as the aerogel thickness increases in 10 mm to 40 mm, the transmittance of the silica aerogel layer decreases from 95.9% to 87.0%. However, when silica particles diameter d changes to 9 nm, the

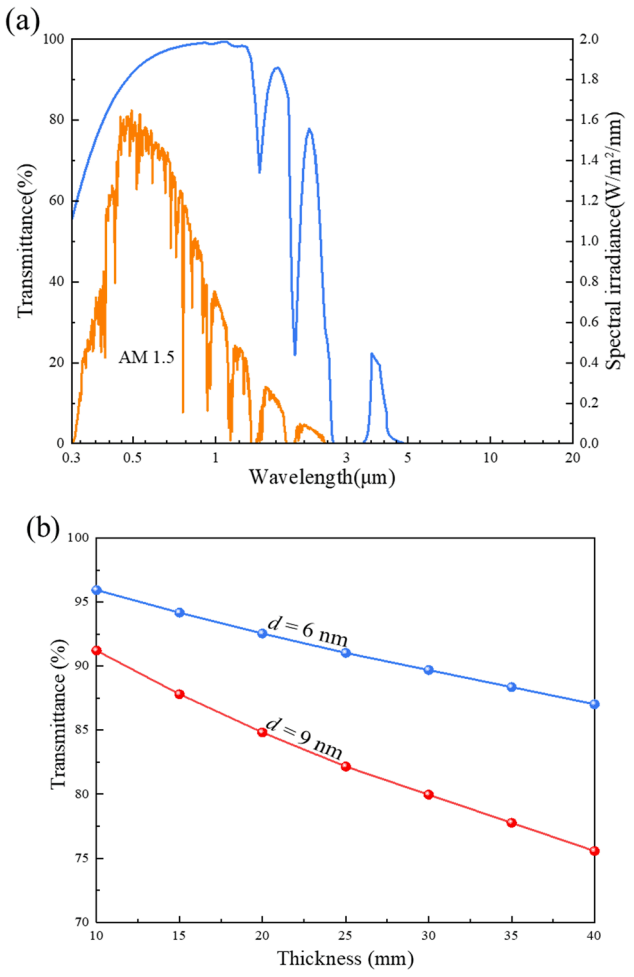

Fig. 5. (a) The direct-hemispherical transmittance spectrum of the aerogel with a thickness of 20 mm and $d = 6$ nm. (b) The transmittance of aerogel at $d = 6$ nm and $d = 9$ nm were plotted.

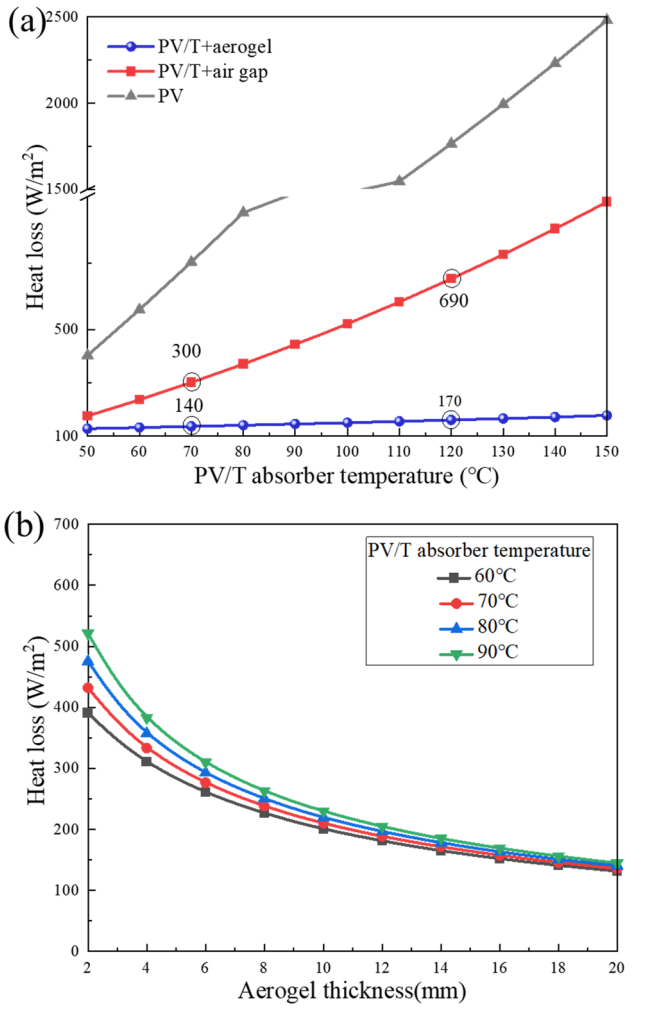

Fig. 6. (a) The heat loss of the aerogel-based PV/T collector, the traditional PV/T collector, and the stand-alone PV module. (b) The heat loss of the aerogel-based PV/T collector at different aerogel thicknesses.

transmittance of the silica aerogel layer decreases from 91.2% to 75.6% when the aerogel thickness increases from 10 mm to 40 mm. This difference is because more solar radiation is scattered or absorbed by the aerogel as the thickness silica aerogel layer and the diameter of the silica particles increases. According to the results, if the thickness of the aerogel layer and diameter of silica particles are respectively set as 15 mm and 6 nm, the transmittance of the silica aerogel can be 94.2%, which indicates that the transmittance of the aerogel can be designed to be equivalent to that of glass.

3.2. Heat loss of the aerogel-based PV/T collector

The heat loss of the aerogel-based PV/T collector, traditional PV/T collector, and the stand-alone PV module is calculated and shown in Fig. 6(a). During the simulation, T_{amb} is set at 25°C. Heat loss is the sum of convection/conduction loss and radiation loss. For simplicity, the convective heat transfer coefficient between the surface of collectors and environment is assumed as a constant of $h = 10$ W/m^2/K, and this is a commonly selected value in the reported cases (Gallandat et al., 2017) for natural convection in the air. The results present that compared with the other two types of collectors, the heat loss of the aerogel-based PV/T collector is significantly reduced. For example, at a temperature (70°C), the heat loss of the traditional PV/T collector is 2.1 times that of the aerogel-based PV/T collector. The above results indicate that the heat loss is suppressed significantly by the silica aerogel.

The heat loss from the PV/T absorber at different aerogel thicknesses is also presented in Fig. 6(b). At the same aerogel thickness, the heat loss raises with the increase of the PV/T absorber temperature since the temperature difference between the environment and the PV/T absorber increases. Besides, heat loss drops with the increased aerogel thickness due to the decreased heat transfer coefficient between the environment and the PV/T absorber. However, it is noted that the increased thickness of the silica aerogel will damage the high solar transmittance of the aerogel layer, thus the effect of the thickness of the aerogel on the overall exergy efficiency of the aerogel-based PV/T is further explored and the results are shown in Fig. 7. As shown in Fig. 7(a), there exists an optimal thickness of the aerogel for a specific PV/T absorber temperature. For example, when the PV/T absorber temperature is 60°C, the optimal thickness of the aerogel layer is approximately 20 mm. Moreover, the optimal aerogel thickness increases with the raising PV/T absorber temperature (Fig. 7(b)) and this is due to that minimizing the heat loss is important at high operating temperatures.

3.3. Thermodynamics analysis of the aerogel-based PV/T collector

Fig. 8(a) illustrates the electrical and thermal efficiencies of the PV/T collector where the aerogel thickness is 20 mm. When the temperature of the PV/T absorber increases from 40°C to 70°C, the thermal efficiency of the aerogel-based PV/T collector drops from 60.0% to 57.1% while that of the traditional PV/T collector decreases from 57% to 39.1%, which shows that the aerogel-based PV/T thermal efficiency is much

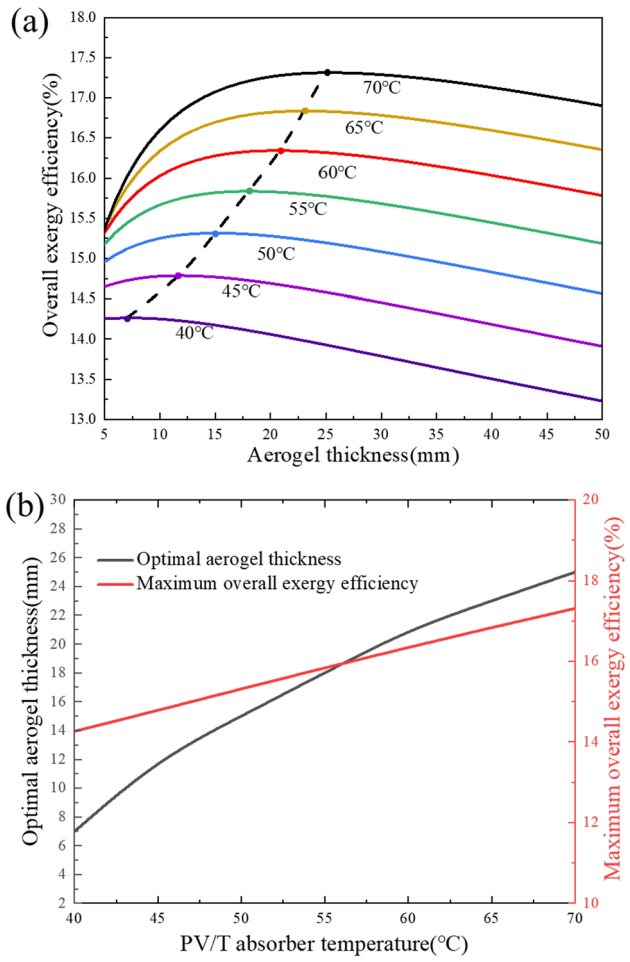

Fig. 7. (a) The overall exergy efficiency of the aerogel-based PV/T collector varies with the thickness of the aerogel (b) Optimal aerogel thickness and maximum overall exergy efficiency.

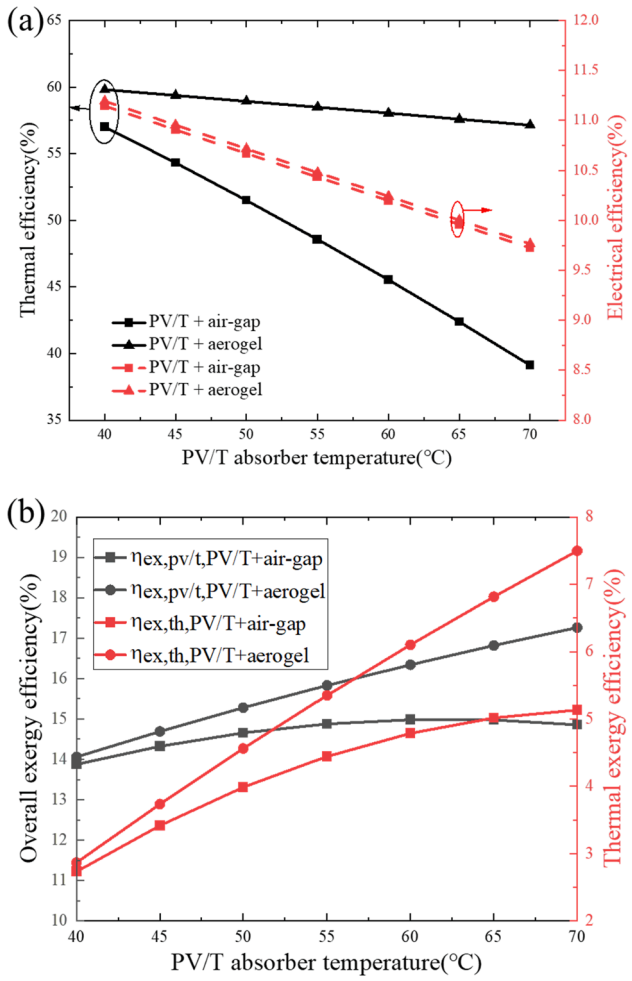

Fig. 8. (a) The thermal and electrical efficiency of two types of collectors.. (b) The exergy efficiency of two types of collectors.

higher than that of the traditional PV/T collector, especially at a higher temperature. The main reason is that the aerogel is opaque to the mid-infrared radiation and the aerogel can absorb the radiation from the PV/T absorber and re-emitted part of it back to the PV/T absorber, thus the radiation loss of the PV/T absorber can be minimized, which greatly contributes to the overall efficiency of the collector. Besides, the electrical efficiency of the aerogel-based PV/T collector is higher than that of the traditional PV/T collector due to the high transmittance of the aerogel. As shown in Fig. 8(a), the electrical efficiency is also affected by the operating temperature of the PV/T absorber, and this scenario depends on the physical properties of the PV cell. If PV cells with a positive temperature coefficient (Huang et al., 2019) are used, the electrical efficiency will be further improved by high operating temperature and this is a good feature for PV/T collectors.

Fig. 8(b) presents the overall exergy efficiency and thermal exergy efficiency of the aerogel-based PV/T collector and the traditional PV/T collector. The aerogel-based PV/T achieves higher overall exergy efficiency at all the operating temperatures since the aerogel prevents heat loss from the hot absorber to the environment. For example, at the operating temperature of 70°C, the overall exergy efficiency of the aerogel-based PV/T collector is 16.2% greater than that of the traditional PV/T collector. Interestingly, the overall exergy efficiency of traditional PV/T collector increases and then drops, reaching a maximum of 15% at the operating temperature of 60°C. However, the overall exergy efficiency of the aerogel-based PV/T collector increases with the rising operating temperature, indicating that the collector can be more efficient at higher temperatures. The overall exergy efficiency of the aerogel-based PV/T collector achieves up to 20.4% at the PV/T absorber temperature of 140°C (beyond the values shown in the plot). Fig. 8(b) presents the thermal exergy efficiency of the two types of collectors, aerogel-based PV/T collector has higher thermal exergy efficiency than the traditional PV/T collector. For example, the thermal exergy efficiency is 1.46 times that of the traditional PV/T collector at the PV/T absorber temperature of 70°C. The overall exergy efficiency of the aerogel-based PV/T collector is also compared to that of PV/T collectors reported in previous studies. (Table 1).

The thermal performance comparison between the aerogel-based PV/T collector and the spectrally selective PV/T collector under different long-wave panel emissivity is presented in Fig. 9, the results show that the thermal efficiency of the spectrally selective PV/T collector decreases with the increases of infrared emissivity of PV cells. When the long-wave panel emissivity of a spectrally selective PV/T collector is 0.1, its thermal efficiency is equivalent to that of an aerogel-based PV/T collector. When the operating temperature is low, the

Table 1
Comparison of the exergy efficiency values between aerogel-based PV/T collector and reported conventional PV/T collectors.

Investigator (s)	PV type	Exergy efficiency (%)
Aberoumand et al. (2018)	Crystalline silicon	11.9–14.2%
Mousavi et al. (2018)	–	16.7%
Wu et al. (2018)	Crystalline silicon	13.8%
Hassani et al. (2016)	Crystalline silicon	11.8%
This study	Poly-crystalline silicon	20.4%

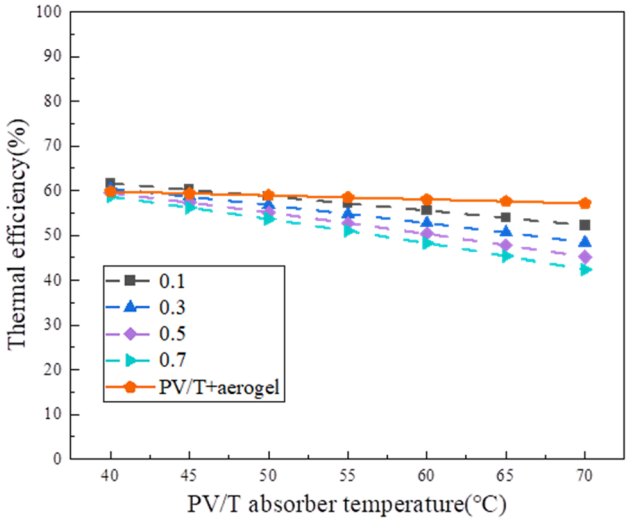

Fig. 9. The thermal performance comparison between the aerogel-based PV/T collector and the spectrally selective PV/T collector under different long-wave panel emissivity.

thermal efficiency of the aerogel-based PV/T collector is a little lower than that of the spectrally selective PV/T collector. On the contrary, when the operating temperature becomes larger, compared with the spectrally selective PV/T collector, the aerogel-based PV/T collector has higher thermal efficiency, because the convective and conductive loss in the spectrally selective PV/T collector became violently.

3.4. Sensitivity analysis

3.4.1. The effect of solar radiation and ambient temperature

Fig. 10(a) illustrates the relationship between the overall exergy efficiency and the thickness of aerogel. The overall exergy efficiency boost then drops with the increase of aerogel thickness and reaches the ceiling at a certain aerogel thickness. For instance, the overall exergy efficiency reaches a maximum value of 17.31% at a thickness of 25 mm. The thermal resistance increases with the aerogel thickness, thermal exergy efficiency increases, so the overall exergy efficiency increases gradually before 25 mm. However, the transmittance of the aerogel decreases with the increasing thickness, and overall exergy efficiency decreases due to optical loss. The optimal aerogel thickness and maximum exergy efficiency at different incident radiation range from 500 to 1000 W/m^2 are plotted in Fig. 10(b). The optimal aerogel thickness decreases gradually with the growing incident radiation, the maximum overall exergy efficiency increases with the raising incident radiation. When the incident radiation increases from 500 W/m^2 to 1000 W/m^2, the optimal aerogel thickness decreases from 44 mm to 25 mm while maximum overall exergy efficiency increases 15.80% to 17.31%. The variation curves of thermal and electrical power with the increase of incident radiation are observed in Fig. 10(c). The amount of electricity and thermal energy is positively linearly correlated with the intensity of incident radiation.

The thermal exergy efficiency and overall exergy efficiency of the aerogel-based PV/T collector at different ambient temperatures are shown in Fig. 11. Thermal exergy efficiency and overall exergy efficiency are functions of ambient temperature and decrease as the ambient temperature increases. As presented in Fig. 11(a), the higher ambient temperature makes the temperature gradient between the PV/T absorber and the environment smaller and then decreases the exergy efficiency. In Fig. 11(b), when ambient temperature boosts from 0°C to 30°C, at the PV/T absorber temperature of 40°C, the overall exergy efficiency of the aerogel-based PV/T collector drops from 19.03% to 13.09%, while the overall exergy efficiency at an operating temperature of 60°C decreases from 21.10% to 15.42%.

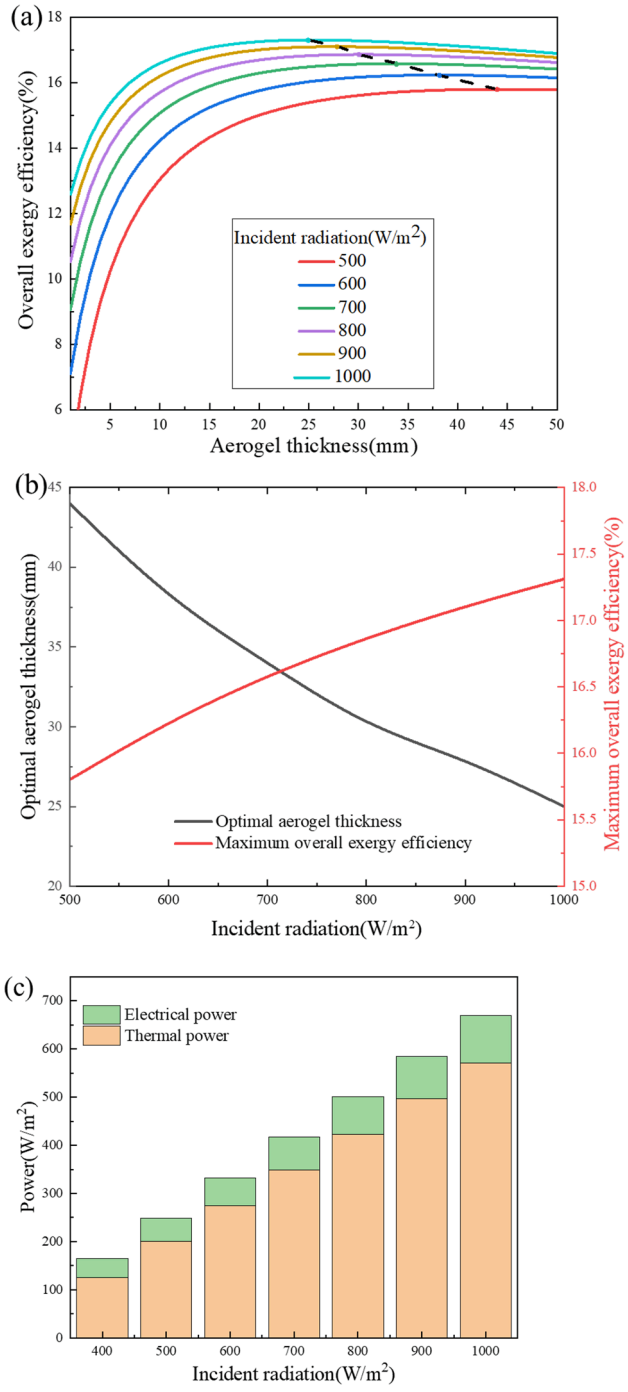

Fig. 10. (a) The overall exergy efficiency of the collector at different aerogel thicknesses. (b) Optimal aerogel thickness and maximum overall exergy efficiency. (c) Electrical and thermal power at different incident radiation.

3.4.2. PV/T absorber emissivity

Theoretically, taking advantage of spectral selective PV/T absorbers is an effective way to suppress heat loss. Here, the performance of aerogel-based collectors with and without the spectral selective PV/T absorber is calculated and analyzed to further demonstrate the influence of the aerogel on the heat collection capacity of aerogel collectors. During the calculation, the values of thermal emissivity of the collector with and without the spectral selective PV/T absorber are set as 0.1 and 0.9, respectively, while the values of solar absorptivity of the two absorbers are set both as 0.9. The comparison results are shown in Fig. 12. The overall exergy efficiency of the aerogel-based PV/T with the spectral

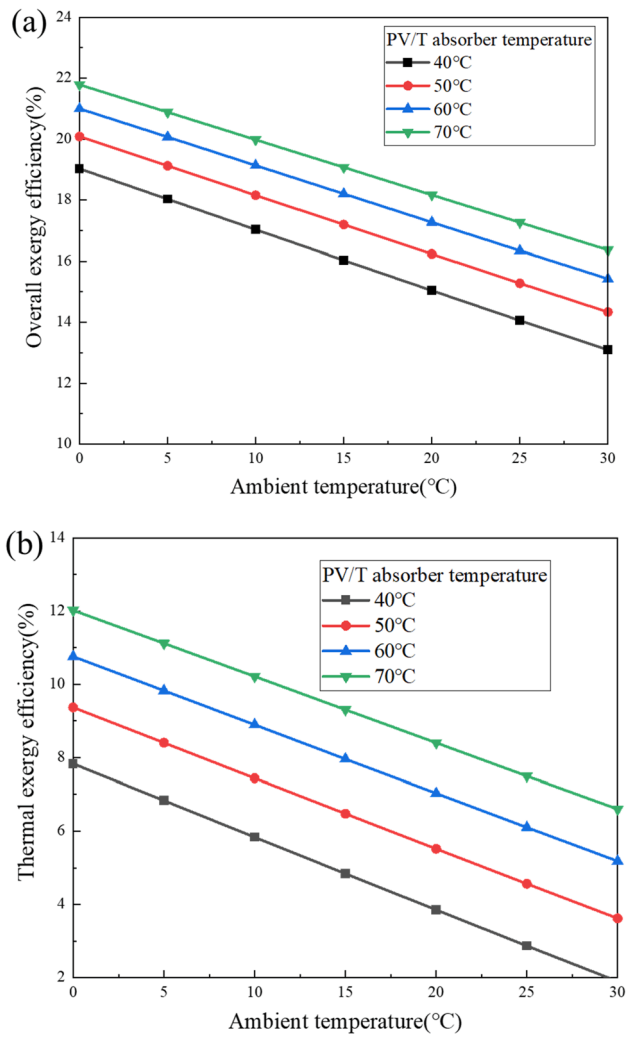

Fig. 11. (a) Overall exergy efficiency. (b) Thermal exergy efficiency under different ambient temperatures.

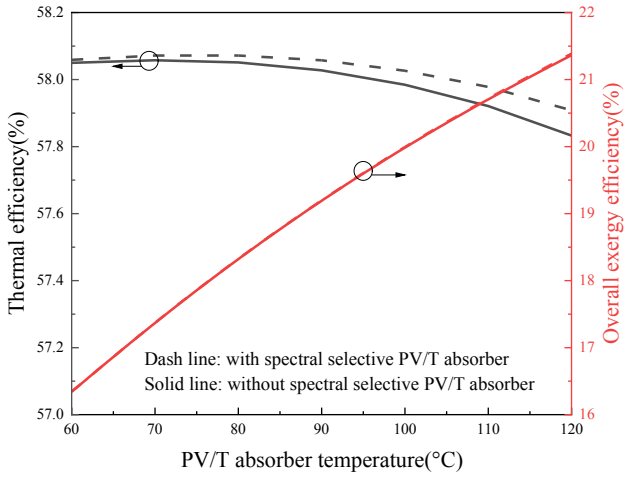

Fig. 12. Effect of the absorber emissivity on the performance of the aerogel-based PV/T collector.

selective absorber is nearly consistent with that of the aerogel-based PV/T without the spectral selective absorber. For instance, with the temperature increases from 60°C to 120°C, the thermal efficiency of the aerogel-based PV/T collector with the spectral selective absorber decreases from 58.06% to 57.91%, while the thermal efficiency of the aerogel-based PV/T without the spectral selective absorber decreases from 58.05% to 57.83%. The overall exergy efficiency of the aerogel-based PV/T collector with the spectral selective absorber increases from 16.34% to 21.39% as the temperature increases from 60°C to 120°C, while the overall exergy efficiency of the aerogel-based PV/T without the spectral selective absorber boosts from 16.33% to 21.36%. These results mean that the emissivity of the PV/T absorber surface has a negligible effect on the aerogel-based PV/T performance, which is a good characteristic for PV/T collectors.

3.5. Economical results

An economic analysis of the aerogel-based PV/T is performed, and the price of the electricity and thermal energy is considered. The output of the aerogel-based PV/T collector is calculated under the climatic conditions of Hefei for domestic hot water applications, so the operating temperature of the aerogel-based PV/T collector is selected as 60°C. The energy price is shown in Table 2 and the costs of equipment, material, and installation of the aerogel-based PV/T are shown in Table 3. Economic savings are estimated based on the investment cost of operating cost savings over 20 years. Results show that the aerogel-based PV/T system (The area of the aerogel-based PV/T collector is selected as 20 m^2) can save 4293.3 USD during the useful life, and the time for the investment recovery of the aerogel-based collector is 11.6 years. It is noted that the thermal and overall exergy efficiencies of the PV/T collector are improved by 46% and 16.7%, respectively, but the total cost of the aerogel-based PV/T collector is just 1.4% high than that of the conventional PV/T collector. The economic saving of the aerogel-based PV/T collector mainly depends on the initial investment. If the government can subsidize the initial investment, it will greatly shorten the time for investment recovery and can significantly increase economic savings. Fortunately, the market for PV/T collectors is constantly growing, and the cost of these systems will be reduced in the future, which is conducive to economic saving.

4. Conclusions

In this paper, a novel PV/T collector is proposed by integrating the optically transparent thermally insulating silica aerogel layer into the PV/T collector to reduce radiative heat loss and improve its performance. An optical-thermal-electrical model is developed for performance analysis of the aerogel-based PV/T collector, including the effect of solar radiation, ambient temperature, and the emissivity of the PV/T absorber. The main conclusions are presented as follow:

(1) The heat loss of the PV/T collector is significantly reduced after introducing silica aerogel into the collector. At a temperature of 70°C, the heat loss of the traditional PV/T collector is 301.1 W/m^2, which is 2.1 times that of the aerogel-based PV/T collector (140.1 W/m^2).

(2) The aerogel-based PV/T collector can get higher thermal and overall exergy efficiencies than those of the traditional PV/T collector. At the temperature of 70°C, the thermal and overall exergy efficiencies of the aerogel-based PV/T collector are 57.1% and 17.3%, respectively, which are 46% and 16.2% higher than those of the traditional PV/T collector.

Table 2
Price of electricity and thermal energy (Lin and Wu, 2017; China Southern Power Grid, 2021).

Electricity price (USD/kWh)	0.1272
Thermal energy price (USD/kWh)	0.05404

Table 3
Cost of the system components (Aguilar-Jiménez et al., 2020; Bhattarai et al., 2013; Xu et al., 2020).

Panels and structure (USD/m^2)	300
Evaluation period (years)	20
Solar tank (USD)	119.34
Installation cost (USD)	1000
Aerogel cost (USD/L)	4

(3) The efficiency of the PV/T collector is significantly influenced by the thermal emissivity of the PV/T absorber. Importantly, the performance of the aerogel-based PV/T collector is equivalent to that of the spectrally selective PV/T collector with a thermal emissivity of 0.1.
(4) At the temperature of 60°C, the thermal efficiency of the aerogel-based PV/T collector without the spectral selective absorber is 58.05%, which is only a little lower than that of the aerogel-based PV/T with the spectral selective absorber (58.06%), indicate that the emissivity of the PV/T absorber surface has a negligible effect on the aerogel-based PV/T performance, which is a good characteristic for PV/T collectors.

In a summary, the silica aerogel-based PV/T collector can suppress the radiative heat loss of the PV/T collector and enhance its solar harvesting performance, which gives a reference for the design of high-performance PV/T utilization.

Declaration of Competing Interest

The authors declare that they have no known competing financial interests or personal relationships that could have appeared to influence the work reported in this paper.

Acknowledgments

This work was supported by the National Natural Science Foundation of China (NSFC 52106276 and 51776193), Project funded by China Postdoctoral Science Foundation (2020TQ0307 and 2020M682033), and the Fundamental Research Funds for the Central Universities (WK2090000028).

References

Aberoumand, S., Ghamari, S., Shabani, B., 2018. Energy and exergy analysis of a photovoltaic thermal (PV/T) system using nanofluids: An experimental study. Sol. Energy 165, 167–177.
Aguilar-Jiménez, J.A., Hernández-Callejo, L., Alonso-Gómez, V., Velázquez, N., López-Zavala, R., Acuña, A., Mariano-Hernández, D., 2020. Techno-economic analysis of hybrid PV/T systems under different climate scenarios and energy tariffs. Sol. Energy 212, 191–202.
Al-Waeli, A.H.A., Sopian, K., Chaichan, M.T., Kazem, H.A., Hasan, H.A., Al-Shamani, A. N., 2017. An experimental investigation of SiC nanofluid as a base-fluid for a photovoltaic thermal PV/T system. Energy Convers. Manage. 142, 547–558.
Benz, N., Beikircher, T.h., Aghazadeh, B., 1996. Aerogel and krypton insulated evacuated flat-plate collector for process heat production. Sol. Energy 58 (1-3), 45–48.
Bhattarai, S., Oh, J.-H., Euh, S.-H., Krishna Kafle, G., Hyun Kim, D., 2012. Simulation and model validation of sheet and tube type photovoltaic thermal solar system and conventional solar collecting system in transient states. Sol. Energy Mater. Sol. Cells 103, 184–193.
Bhattarai, S., Kafle, G.K., Euh, S.-H., Oh, J.-H., Kim, D.H., 2013. Comparative study of photovoltaic and thermal solar systems with different storage capacities: Performance evaluation and economic analysis. Energy 61, 272–282.
Burlafinger, K., Vetter, A., Brabec, C.J., 2015. Maximizing concentrated solar power (CSP) plant overall efficiencies by using spectral selective absorbers at optimal operation temperatures. Sol. Energy 120, 428–438.
China Southern Power Grid. URL <http://www.csg.cn/> (accessed 12.08.2021).
Chow, T.T., Pei, G., Fong, K.F., Lin, Z., Chan, A.L.S., Ji, J., 2009. Energy and exergy analysis of photovoltaic–thermal collector with and without glass cover. Appl. Energy 86 (3), 310–316.
Cox Iii, C.H., Raghuraman, P., 1985. Design considerations for flat-plate-photovoltaic/thermal collectors. Sol. Energy 35 (3), 227–241.
Du, M., Tang, G.H., Wang, T.M., 2019. Exergy analysis of a hybrid PV/T system based on plasmonic nanofluids and silica aerogel glazing. Sol. Energy 183, 501–511.
Dubey, S., Sarvaiya, J.N., Seshadri, B., 2013. Temperature Dependent Photovoltaic (PV) Efficiency and Its Effect on PV Production in the World – A Review. Energy Procedia 33, 311–321.
Ehrmann, N., Reineke-Koch, R., 2012. Selectively coated high efficiency glazing for solar-thermal flat-plate collectors. Thin Solid Films 520 (12), 4214–4218.
Gagliano, A., Tina, G.M., Aneli, S., Nižetić, S., 2019. Comparative assessments of the performances of PV/T and conventional solar plants. J. Cleaner Prod. 219, 304–315.
Gallandat, N., Bérard, J., Abbet, F., Züttel, A., 2017. Small-scale demonstration of the conversion of renewable energy to synthetic hydrocarbons. Sustain. Energy Fuels 1 (8), 1748–1758.
Günay, A.A., Kim, H., Nagarajan, N., Lopez, M., Kantharaj, R., Alsaati, A., Marconnet, A., Lenert, A., Miljkovic, N., 2018. Optically Transparent Thermally Insulating Silica Aerogels for Solar Thermal Insulation. ACS Appl. Mater. Interfaces 10 (15), 12603–12611.
Hassani, S., Saidur, R., Mekhilef, S., Taylor, R.A., 2016. Environmental and exergy benefit of nanofluid-based hybrid PV/T systems. Energy Convers. Manage. 123, 431–444.
He, Y.-L., Xie, T., 2015. Advances of thermal conductivity models of nanoscale silica aerogel insulation material. Appl. Thermal. Eng. 81, 28–50.
Heinemann, U., Caps, R., Fricke, J., 1996. Radiation-conduction interaction: an investigation on silica aerogels. Int. J. Heat Mass Transf. 39 (10), 2115–2130.
Huang, X., Li, W., Fu, H., Li, D., Zhang, C., Chen, H., Fang, Y.i., Fu, K., DenBaars, S.P., Nakamura, S., Goodnick, S.M., Ning, C.-Z., Fan, S., Zhao, Y., 2019. High-Temperature Polarization-Free III-Nitride Solar Cells with Self-Cooling Effects. ACS Photonics 6 (8), 2096–2103.
Ji, J., Luo, C., Chow, T.-T., Sun, W., He, W., 2011. Thermal characteristics of a building-integrated dual-function solar collector in water heating mode with natural circulation. Energy 36 (1), 566–574.
Kalogirou, S.A., Tripanagnostopoulos, Y., 2006. Hybrid PV/T solar systems for domestic hot water and electricity production. Energy Convers. Manage. 47 (18-19), 3368–3382.
Li, Z.-Y., Liu, H.e., Zhao, X.-P., Tao, W.-Q., 2015. A multi-level fractal model for the effective thermal conductivity of silica aerogel. J. Non Cryst. Solids 430, 43–51.
Lin, B., Wu, W., 2017. Economic viability of battery energy storage and grid strategy: A special case of China electricity market. Energy 124, 423–434.
McEnaney, K., Weinstein, L., Kraemer, D., Ghasemi, H., Chen, G., 2017. Aerogel-based solar thermal receivers. Nano Energy 40, 180–186.
Mishchenko, M.I., Travis, L.D., Lacis, A.A., 2002. Scattering, absorption, and emission of light by small particles. Cambridge University Press.
Modest, M.F., 2013. Radiative heat transfer. Academic Press.
Mousavi, S., Kasaeian, A., Shafii, M.B., Jahangir, M.H., 2018. Numerical investigation of the effects of a copper foam filled with phase change materials in a water-cooled photovoltaic/thermal system. Energy Convers. Manage. 163, 187–195.
Palik, E.D., 1998. Handbook of optical constants of solids. Academic Press.
Ren, X., Li, J., Gao, D., Wu, L., Pei, G., 2021. Analysis of a novel photovoltaic/thermal system using InGaN/GaN MQWs cells in high temperature applications. Renew. Energy 168, 11–20.
Strobach, E., Bhatia, B., Yang, S., Zhao, L., Wang, E.N., 2017. High temperature annealing for structural optimization of silica aerogels in solar thermal applications. J. Non Cryst. Solids 462, 72–77.
Tang, G.H., Bi, C., Zhao, Y., Tao, W.Q., 2015. Thermal transport in nano-porous insulation of aerogel: Factors, models and outlook. Energy 90, 701–721.
Tang, A.-M., Cui, Y.-J., Le, T.-T., 2008. A study on the thermal conductivity of compacted bentonites. Appl. Clay Sci. 41 (3-4), 181–189.
van Helden, W.G.J., van Zolingen, R.J.C., Zondag, H.A., 2004. PV thermal systems: PV panels supplying renewable electricity and heat. Prog. Photovoltaics Res. Appl. 12 (6), 415–426.
Wolf, M., 1976. Performance analyses of combined heating and photovoltaic power systems for residences. Energy Convers. 16 (1-2), 79–90.
Wu, S.-Y., Chen, C., Xiao, L., 2018. Heat transfer characteristics and performance evaluation of water-cooled PV/T system with cooling channel above PV panel. Renew. Energy 125, 936–946.
Xu, Z., Zhang, L., Zhao, L., Li, B., Bhatia, B., Wang, C., Wilke, K.L., Song, Y., Labban, O., Lienhard, J.H., Wang, R., Wang, E.N., 2020. Ultrahigh-efficiency desalination via a thermally-localized multistage solar still. Energy Environ. Sci. 13 (3), 830–839.
Yu, Q., Hu, M., Li, J., Wang, Y., Pei, G., 2020. Development of a 2D temperature-irradiance coupling model for performance characterizations of the flat-plate photovoltaic/thermal (PV/T) collector. Renew. Energy 153, 404–419.
Zhao, L., Yang, S., Bhatia, B., Strobach, E., Wang, E.N., 2016. Modeling silica aerogel optical performance by determining its radiative properties. AIP Adv. 6 (2), 025123. https://doi.org/10.1063/1.4943215.
Zhao, L., Bhatia, B., Yang, S., Strobach, E., Weinstein, L.A., Cooper, T.A., Chen, G., Wang, E.N., 2019. Harnessing Heat Beyond 200 degrees C from Unconcentrated Sunlight with Nonevacuated Transparent Aerogels. ACS Nano 13 (7), 7508–7516.
Zhao, L., Bhatia, B., Zhang, L., Strobach, E., Leroy, A., Yadav, M.K., Yang, S., Cooper, T. A., Weinstein, L.A., Modi, A., Kedare, S.B., Chen, G., Wang, E.N., 2020. A Passive High-Temperature High-Pressure Solar Steam Generator for Medical Sterilization. Joule 4 (12), 2733–2745.